Semi-empirical evaluation of PEMFC electro-catalytic activity

P. Spinelli [a,*], C. Francia [a], E.P. Ambrosio [a], M. Lucariello [b]

[a] *Dipartimento di Scienza dei Materiali e Ingegneria Chimica, Politecnico di Torino, Corso Duca degli Abruzzi 24, 10129 Torino, Italy*
[b] *HYSYLAB, Environment Park, Via Livorno 60, 10143 Torino, Italy*

Abstract

The investigation of the performance of small single PEMFC was carried out by employing a purposely designed test bench with complete control of the operational parameters. A MEA preparation method was also developed constituting the base for testing new electrocatalytic materials or improved electrode assembling techniques. Beyond determining the polarization curves, other tests have been carried out like electrical resistance measurement by the current interruption method and voltammetric characterization. A semi-empirical approach based on a simplified mathematical model has been used to fit the experimental polarization data, providing useful parameters for evaluating the electrocatalytic activity together with other significant data of the MEA performance. The analysis of polarization curves includes the determination of the OCV by considering the mixed potential at the oxygen electrode by fitting the initial data with an arbitrary oxidation reaction. This can provide an estimate of hydrogen crossover. Possible change of ohmic resistance with current intensity is discussed. The preliminary results, demonstrating the feasibility of the method are reported.

1. Introduction

Since the introduction of proton exchange membrane fuel cell (PEMFC) technology, whose significant advantages as power sources started to be recognized in the 80s, a vast amount of work has been carried out to understand the basic features and to optimize the design of such promising system. The wide literature available which has been very well reviewed in excellent papers [1–4], provides the understanding of the complex phenomena governing the operation of PEMFC. All the energetic losses have been extensively investigated with particular attention to the kinetics of the electrochemical reactions, the ohmic losses in both ionic and electronic conductors, the mass transfer limitations of the gases. Many studies have been carried out by means of electrochemical methods with small electrodes in laboratory cells, mainly to investigate the catalytic effect of the electrochemical reactions. These studies provide valuable knowledge of the basic phenomena but cannot be easily transferred to describe the overall behavior of the fuel cell due to the

complexity of the membrane-electrode-assembly (MEA) system. On the other hand, testing of complete cells gives in a simple way the performance of the entire system, but does not easily consent the separate determination of the various energetic losses. A remarkable research effort concerning new or modified electrocatalysts has been done in recent years [5–10] devoted to the cost and catalytic activity issues in addition to fundamental research [11–15].

The need for a common basis of the two different experimental approaches is mandatory when the object of the investigation is the efficiency of the catalytic layer of the real MEA, because the presence of important losses different from those connected with the electro-catalytic behavior can mask the required information on this last effect. To this end, the evaluation of the different losses: activation overpotentials, concentration overpotentials, ohmic losses, must be obtained from the overall polarization curve.

Starting from these considerations, our group initiated a research project to investigate possible improvements of the electrode catalytic layer in the MEA.

To this purpose, a complete test bench for small single PEMFC or stacks up to about 100 W has been designed together with a test methodology aimed at the evaluation of the catalytic

---

* Corresponding author. Tel.: +39 0115644643; fax: +39 0115644699.
E-mail address: paolo.spinelli@polito.it (P. Spinelli).

layers of various MEAs by separately determining the activation overpotential and the other losses. A standard procedure has been also set up for the preparation of MEAs for the testing of new electrocatalytic materials or new assembling techniques. A simplified yet effective treatment for the analysis of the experimental data has been also developed, whose preliminary results are reported in the present contribution. The semi-empirical analysis of polarization curves presented here is quite different from similar treatment found in the literature [20–24]. Some of the points which render the present approach different with respect to the cited literature are (i) complete Butler–Volmer equations for both the cathode and the anode, instead of Tafel approximation, (ii) the open circuit voltage is computed as a mixed potential by assuming an arbitrary oxidation current at the cathode, (iii) an expression for ohmic resistance as a function of current intensity is introduced to account for phenomena which require a more sophisticated treatment, such as increase of membrane resistance with current due to partial de-hydration on the anodic side, or non-ohmic effects due to the porous 3D nature of the electrodes.

The approach presented in this paper has been applied to hydrogen PEMFC, but it can be used for other MEA based fuel cells, such as DMFC for which the need to improve the performance of the catalytic layer is even more stringent.

2. Experimental

The tests have been carried out on commercial single cells (ElectroChem Inc.) of two different size (1.4 W, 5 cm^2 and 14 W, 50 cm^2). The cells were assembled both with the commercial MEA provided by the supplier (Nafion® 115 as the polymeric membrane, with a platinum loading of 1 mg cm^{-2}, 20 wt.% Pt/C on Vulcan XC-72 catalyst, carbon papers as gas diffusion layers) and with MEAs prepared in the laboratory.

The MEA preparation process, derived from the literature on the subject [3,16–18], starts with painting the catalyst ink on both sides of the Nafion® membrane. The membranes were pre-treated by boiling for 30 min at 80 °C in 7 M HNO$_3$ solutions, 5% H$_2$O$_2$, 1 M H$_2$SO$_4$ and distilled water consecutively. The procedure assured the complete removal of the organic and metallic impurities which might be present on the membrane surface. Prior to the electrode preparation the membranes were dried and flattened. The catalyst ink was prepared by mixing supported platinum catalyst (20 wt.% Pt supported on Vulcan XC-72R, ElectroChem Inc.) and Nafion (5% wt solution, ElectroChem Inc.) in isopropyl alcohol (Aldrich) and water 1:1. The weight ratio between Pt/C and Nafion was 7:3.

The membrane-electrode-assembly obtained was hot-pressed between two teflonised carbon cloths (ElectroChem Inc.) at a pressure of 50 MPa for 2 min, at 115 °C.

The PEMFC test bench used for the cell management has been purposely designed. It presents, with respect to the available commercial units, important improvements. One of these regards the possibility of controlling the amount of water in the gas humidifying process by means of two separate pumps dosing the water to be added, after proper vaporization, to the hydrogen and oxygen feeds. Thus, the amount of water in the

gases is independent of the temperature, being limited only by the saturation pressure at the operating temperature. Moreover, the complete water balance can be determined by collecting, as liquid phase, all the water coming out from the cell. All the settings of the test bench concerning gases flow, temperature, humidity are controlled by an automated system connected to a computer, which also allows the acquisition of the test data.

Commercial and laboratory prepared MEAs were fed with humidified H$_2$ and O$_2$ (usually 100% RH) gases at atmospheric pressure; the stoichiometry flow of pure H$_2$ and O$_2$ was usually 2; the operating temperature of the cell was set in the range 70–80 °C. All the cells to be tested were initially subjected to a conditioning procedure to equilibrate the water content inside the membrane. Two different procedures have been used, the first one, frequently reported in the literature, consists in holding the cell at a voltage of 0.6 V for at least 2 h until a steady value of the current intensity is obtained; the second conditioning procedure, which is the one we used for the tests presented in this work, consists in performing cyclic, slow rate (0.2 mV s^{-1}), polarization curves from the OCV to 0.4 V and reverse, until (typically from 10 to 20 cycles) the curve itself does not change any longer. For both procedures the cell is operated with humidified H$_2$ and dry O$_2$, with stoichiometry flows of 2.

The value of the ohmic resistance of the cell was determined by the method based on current interruption [19], employing the electrochemical AMEL 5000 system which allows the recording of the cell voltage after current interruption with a sampling time as short as 10 μs. The apparatus is a complete galvanostat/potentiostat with a built in micro-processor and DMA features for the recording of fast transient. This technique provides a direct reproducible measurement of the electrical resistance of the membrane and electronic conductors. The only limitation in the present equipment is the maximum output current of 1 A. So we use the apparatus for precise determination of the ohmic resistance at low currents, while the polarization tests are carried out by another power supply operating both at constant current and voltage. A modification of the power supply system to perform resistance measurements by the current interrupt method at higher currents is under development.

The polarization curves of the cells were obtained by applying a sequence of constant current steps, starting from zero and increasing the current at each step, after reaching the stationary value of the cell voltage, which typically occurs in a few minutes (from 5 to 10) averaging the voltage values during the last minute. In some cases we have also employed a slow potentiodynamic technique, by varying the cell voltage at rates between 0.2 and 1 mV s^{-1}, the results of numerous experiments indicated no significant difference between the two techniques, the second one allows to increase the number of experimental points in the first part of the polarization curve, which is important for the analysis described in the following section.

3. Analysis of polarization curves

In order to analyze the behavior of the MEA, particularly to obtain the information about the catalytic activity, a simplified

model has been developed by which the computed polarization $V(I)$ curve is obtained and compared with the experimental data.

This simplified model takes into account the electrochemical kinetics of hydrogen and oxygen reactions by considering the Butler–Volmer equation for both processes, employing a reference value for the exchange current density for hydrogen and oxygen (referred to 1 cm^2 of geometric MEA surface) derived from literature data and the values of the transfer coefficients. The limitations due to mass transfer of the gas reagents to the electrodes are introduced in the model through the values of the limiting currents for hydrogen and oxygen, which in turn depend on the stoichiometric coefficients of the gases under the test conditions. Moreover the value of the electrical resistance due to ohmic drop in the membrane and in the electronic conductors is considered. For the polarization curves analyzed in this paper, the ohmic resistance is computed starting from the experimental value obtained by the current interruption technique.

The analysis of the experimental polarization curve is carried out in subsequent steps by considering the various contributions according to the relationship:

$$V(i) = E_{rev} - (\eta_{act,O_2} + \eta_{act,H_2} + \eta_{conc,O_2} + \eta_{conc,H_2} + Ri) \quad (1)$$

where activation and concentration overpotentials are considered in absolute value. The computation takes into account the formation of a mixed potential at open circuit, providing the value $V(0) < E_{rev}$, as discussed in the following.

3.1. Activation overpotential

To compute the relationship between activation overpotential and current density for both oxygen reduction and hydrogen oxidation, the well known Butler–Volmer equation is used:

$$i = i_0 \left[\exp\left(\alpha_{an}\frac{F}{RT}\eta \right) - \exp\left(-\alpha_{cat}\frac{F}{RT}\eta \right) \right] \quad (2)$$

where i_0 is the exchange current density and $\alpha_{an} = \beta z$, $\alpha_{cat} = (1 - \beta)z$ are the transfer coefficient for the anodic and cathodic branch of the $i(\eta)$ curve for the given electrochemical reaction. According to the basic definitions in electrochemical kinetics, β is the so called "symmetry factor" and z the number of electrons transferred in the overall process. The other symbols have the usual meaning.

In our analysis, Eq. (2) is applied differently for oxygen reduction and hydrogen oxidation.

For the oxygen reduction reaction, both i_0 and α_{cat} are obtained by fitting the experimental data because, due to the extremely low value of the exchange current density, even for very low values of current density, the negative activation overpotential η is sufficiently high to render negligible the first term in Eq. (2). Thus, the first part of the polarization curve, up to about 5 mA cm^{-2}, can easily be fitted on the semi-logarithmic plot $V/\log(|I|)$ by the linear Tafel equation: $\eta = a - b \log(|I|)$, where the two fitting parameters a and b, which correspond to the position and slope of the Tafel line, provide the values for i_0 and α_{cat}, respectively. Thus, rearranging Eq. (2) by neglecting

the first exponential term, we obtain:

$$\ln|i| = \ln i_0 - \frac{\alpha_{cat}F}{RT}\eta \quad (3)$$

$$\eta = \frac{RT}{\alpha_{cat}F}\ln i_0 - \frac{RT}{\alpha_{cat}F}\ln|i| \quad (4)$$

$$\eta = a - b\log|i| \quad (5)$$

$$b = \frac{-2.03\,RT}{\alpha_{cat}F}, \qquad a = -b\log(i_0) \quad (6)$$

This is illustrated in Fig. 1; at first a tentative value $\alpha_{cat} = 1$ is used allowing the determination of a first approximation value of i_0. Then, the best fitting for both parameters is carried out in a few iteration steps. It is important to note that in the range where the Tafel linear trend holds, only the activation overpotential for ORR is considered, the other terms being negligible, so the b and i_0 values for ORR are derived independently of the other fitting parameters, which will be obtained in subsequent steps.

Also for the hydrogen oxidation reaction, Eq. (2) is used, but one fitting parameter only, the exchange current density, is introduced, while the values of the transfer coefficients are taken from literature data. This procedure is necessary because of the lack of a linear portion of the experimental data attributable to the HOR alone. It must be noted that due to the relatively high value of i_0 for hydrogen oxidation, compared to the one for the ORR, the above procedure appears adequate to the scope of the analysis. In fact, the estimation of the exchange current density for HOR is obtained by fitting the experimental data in the part of the polarization curve where ohmic and concentration polarization are negligible. Fig. 2 illustrates this point. Curve a on this figure is the computed curve for the activation overpotential of oxygen reduction as previously indicated, curve b is the sum of activation overpotentials for oxygen reduction and hydrogen oxidation, this last being the difference between curve b and a, the open circles are the experimental points (curve c). The open circuit volt-
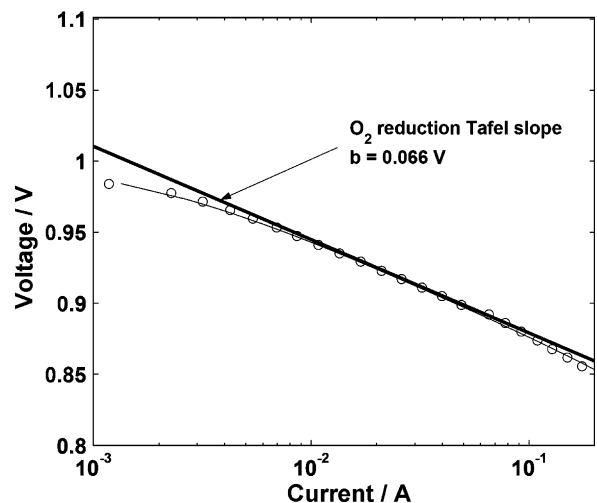

Fig. 1. Determination of the exchange current density i_0 and cathodic transfer coefficient α_{cat} for the ORR, by linear fitting of the first part of the polarization curve corresponding to Test 2 reported in Fig. 7. Laboratory prepared MEA, 0.5 mg Pt cm^{-2}, geometric surface 5 cm^2, $T = 70\,°C$, humidified H$_2$ and O$_2$ (100% RH) at atmospheric pressure, stoichiometry flow 2.
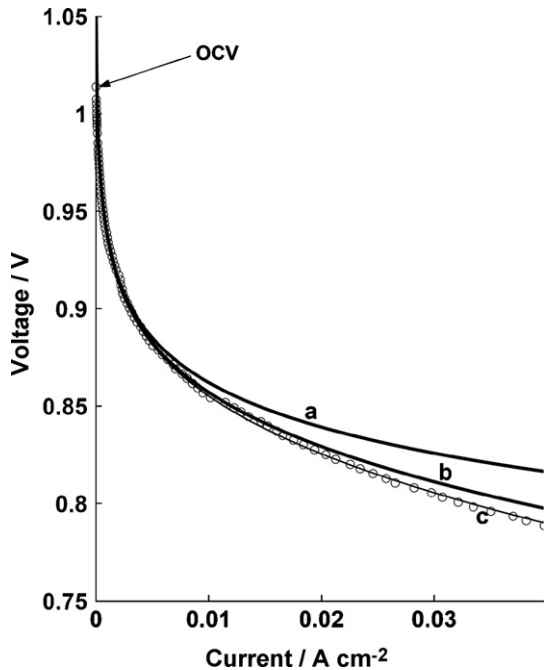
Fig. 2. Computed curves for the activation overpotential of the oxygen reduction and hydrogen oxidation reactions for a laboratory prepared MEA, 0.5 mg Pt cm^{-2}, geometric surface 5 cm^2, $T = 70\,^\circ$C, humidified H$_2$ and O$_2$ (100% RH) at atmospheric pressure, stoichiometry flow 2. Curve a ($E_{rev} - \eta_{act,O_2}$) is the computed curve for the activation overpotential of oxygen reduction, curve b ($E_{rev} - \eta_{act,O_2} + \eta_{act,H_2}$) is the sum of activation overpotentials for oxygen reduction and hydrogen oxidation, the open circles are the experimental points (curve c). The open circuit voltage is shown on the graph (OCV), while the reversible voltage ($E_{rev} = 1.19$ V in this test) is not reported to improve the readability of the graph. Concentration overpotentials and ohmic drop are negligible on this graph.

age is shown on the graph (OCV), while the reversible voltage (1.19 V in this test) is not reported to improve the readability of the graph. It can be seen that curve a ($E_{rev} - \eta_{act,O_2}$) departs from the experimental data at about 5 mA cm^{-2}, while curve b ($E_{rev} - \eta_{act,O_2} - \eta_{act,H_2}$) fits the data up to about 15 mA cm^{-2}. To obtain a good fitting of this part of the curve, accounting for the activation overpotential for hydrogen oxidation, a high number of experimental points is necessary at the beginning of the polarization curve.

3.2. Open circuit voltage

It is frequently reported in the literature regarding the modeling of single PEMFC that the values of open circuit voltage markedly differ from those computed from the equilibrium (Nernst) equation. It is commonly accepted that those differences are attributable to the oxygen electrode, for which equilibrium conditions cannot be attained at open circuit. Since the basic studies by Conway, Bockris, Hoare, Damjanovic and others, for a review of the topic see Ref. [25], the reasons for this behavior were interpreted in terms of parasitic reactions responsible for a mixed-potential conditions. Among the various parasitic reactions which have been assumed, those which received major attention are Pt or electrode surface oxidations and hydrogen peroxide reactions. In addition to these reactions,

which occur independently of the other electrode of the system, an important effect on the open circuit potential is observed in PEM fuel cell, when possible crossover of hydrogen through the membrane is considered. In this case, an oxidation current for hydrogen at the cathode has been considered. The effects of hydrogen crossover have been investigated by various authors [26–31].

In our simplified approach the above phenomena are taken into consideration by assuming an arbitrary oxidation current which should include all possible causes. This is schematically illustrated in Fig. 3, where the fitting of experimental data at low current densities is obtained by using such an empirical approach.

On this graph, the circles are the experimental point. The fuel cell reversible voltage and the open circuit voltage due to the mixed potential are shown. The "parasitic oxidation reaction" curve is arbitrary and corresponds to best-fitting values of the equation:

$$V_s = V_{s0} + c_s \frac{RT}{F} \log\left(\frac{I_s}{I_{ls} - I_s}\right) \qquad (7)$$

where V_s and I_s are the voltage/current values for the parasitic reaction(s), V_{s0} the half-wave potential of the curve, c_s an empirical coefficient accounting for the curve slope and I_{ls} is the limiting value for the oxidation reaction. Even if the fitting by using three parameters appears awkward, it can be observed that the sensitivity of those parameters is such that best fitting conditions can be obtained easily. Though this fitting, aiming at finding the value of the open circuit voltage, is practically independent of the fitting parameters corresponding to the other dissipation sources (oxygen and hydrogen activation overpotentials, ohmic contributions and concentration overpotentials), it is more easily accomplished if the activation overpotential for ORR has already been carried out.
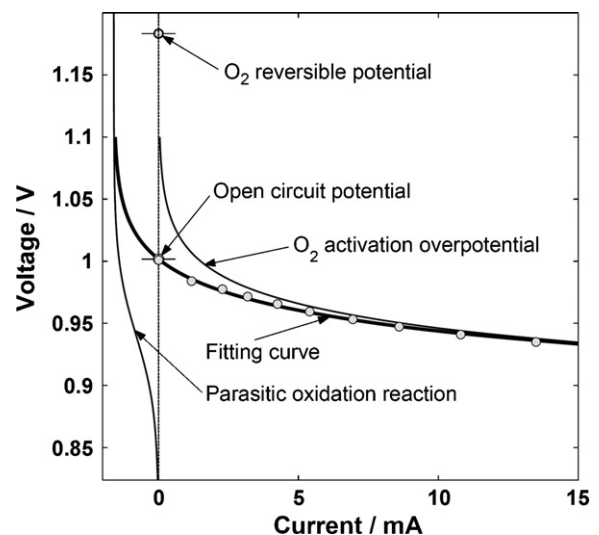

Fig. 3. Mixed potential analysis of the polarization curve at very low current density to obtain a curve fitting starting from the open circuit voltage. The computation provides an estimation of hydrogen crossover from the value of the current of the parasitic reaction at the OCV. The data refer to the same test shown in Figs. 1 and 2.

An interesting result from this computation is the value of the current density for the parasitic reactions at the open circuit potential. This current is mainly due to the hydrogen crossover oxidation and in many experiments [26,27] carried out with Nafion® membranes at 70 °C ranges from 0.2 to 0.5 mA cm^{-2}. These data are in good agreement with our computed values.

3.3. Concentration overpotential

Concentration overpotential arises from the concentration gradient which is established when a given current flows within an electrochemical cell due to the consumption of reagents at the electrode surface and the consequent mass transfer (diffusional) mechanism to replace them. The simplest way to express this type of overpotential is to consider the value of the limiting current density corresponding to the flux of reagent supplied to the system.

In case of gaseous reagents such as oxygen or hydrogen, if we know the flux (e.g. q_{H_2} mol s^{-1} cm^{-2}), then the current corresponding to such a flux, $|i_l| = 2Fq_{H_2}$ A cm^{-2}, is the maximum possible value, i.e. the limiting current density. If we consider concentration overpotential alone, by neglecting all other dissipation terms, the relationship between overpotential and current density is easily obtained:

$$|\eta_{conc}| = -\frac{RT}{zF}\ln\left(1 - \frac{i}{i_l}\right) \tag{8}$$

By considering the absolute value of the overpotential, such a relationship is valid for both cathodic and anodic reactions, because the logarithmic expression is always negative.

If we apply Eq. (8) to the hydrogen oxidation reaction we obtain:

$$|\eta_{conc}|_{H_2} = -\frac{RT}{2F}\ln\left(1 - \frac{i}{i_{l,H_2}}\right) \tag{9}$$

and for oxygen reduction:

$$|\eta_{conc}|_{O_2} = -\frac{RT}{4F}\ln\left(1 - \frac{i}{i_{l,O_2}}\right) \tag{10}$$

This approach avoids complex calculations of concentration or pressure profiles of reagents, because it is based on the assumption that mass transfer limitation is described by the concentration gradient $(\partial C/\partial x)_{x=0}$ at the electrode surface, whose maximum value is proportional to the limiting current.

Even if the real situation in 3D electrodes is much more complex, the above equations are applicable for the scope of the present work.

In the analysis of polarization curves, it must be observed that usually the flow of gaseous reagents is set to a value described by the so called stoichiometric coefficient λ_i, that is the ratio between the flow of reagent fed to the system and the flow corresponding to the applied current. Since this condition requires a change of the reagent feed with current to keep the stoichiometric coefficient constant during the polarization test, commonly the stoichiometric coefficient is referred to the maximum value of the applied current. Under these conditions, the limiting current value is: $i_l = \lambda_i i_{max}$. Under these simplifying conditions, the

computation of the concentration overpotential does not require the determination of fitting parameters.

3.4. Ohmic dissipation

The computation of the voltage drop due to the ohmic resistance of the membrane and electrodes, could be simply considered as the product RI, where the resistance value R, fitting the experimental polarization curve, fairly agrees with the measured ohmic resistance.

It was observed that in the majority of polarization curves analyzed, this term is insufficient to provide a good fitting of the experimental data, especially when the test is carried out at rather high values of current density (above 1 A cm^{-2}).

It was found that a very good fitting can be obtained by considering a change of the ohmic resistance with current intensity, $R = R(I)$. This assumption is consistent with the findings of various authors [24,32–34] who interpret the increase of the membrane resistance with increasing current intensity as a consequence of a partial de-hydration at the anode side due to electroosmotic drag. It is worth noting that the change of resistance with current is supported by experimental measurements of the ohmic resistance both by the current interruption method and by electrochemical impedance [32,33].

We assume the following relationship: $R(I) = R_0(1 + aI^n)$, where R_0 is adjusted starting from the experimental resistance value determined at low current density (about 0.2 A cm^{-2}) and the parameter a is obtained by fitting; n is close to 1, but can be adjusted (typically from 0.9 to 1.1) for a better fitting.

Fig. 4 illustrates the determination of the ohmic resistance by the current interrupt technique for the laboratory prepared MEA described in the caption. The current before interruption was 0.998 A, the obtained resistance value is 0.24 Ω cm^{-2},
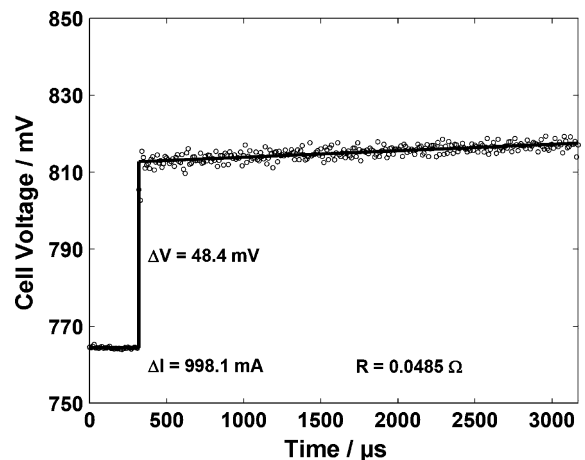
Fig. 4. Determination of ohmic resistance by the current interrupt technique for the laboratory prepared MEA, 0.5 mg Pt cm^{-2}, geometric surface 5 cm^2, $T = 70$ °C, humidified H$_2$ and O$_2$ (100% RH) at atmospheric pressure, stoichiometry flow 2. The test starts at a voltage of 0.764 V with a stabilized current of 0.998 A. After interruption by a fast solid state switch (<1 μs) the current goes to zero and the voltage abruptly increases. To obtain the resistance, the voltage change is computed as indicated in the figure by linear regression of the experimental point after interruption. The sampling time is 10 μs. The measured resistance value of 0.0485 Ω gives a specific resistance of 0.24 Ω cm^{-2}.

Table 1
Results obtained by analyzing the polarization curves reported in Fig. 7

Polarization curve (Fig. 7)	Cathode exchange current density (A cm^{-2})	Anode exchange current density (A cm^{-2})	Cathodic transfer coefficient	$R_{average}$ (Ω cm^{-2})	Catalytic activity $i_{\eta=0.3}$ (mA cm^{-2})	Current for hydrogen crossover (mA cm^{-2})
Test 1	8.0×10^{-7}	4.5×10^{-2}	0.94	0.59	8.52	0.18
Test 2	5.3×10^{-7}	5.0×10^{-2}	1.0	0.26	19.2	0.28
Test 3	1.0×10^{-6}	7.0×10^{-2}	0.99	0.18	17.4	0.34

which fairly well agrees with the average value of 0.26 Ω cm^{-2}, obtained by fitting the polarization curve (Test 2 in Fig. 7, see also the data reported in Table 1) by the $R(I)$ expression above described.

Due to the choice of the mathematical relation to express the change of resistance with current, the computation is carried out with the values of the total cell resistance and current intensity. Then the resistance referred to unit of geometric surface of MEA is obtained. It must be observed that the term $R(I)$ can include non-ohmic effects due to the porous 3D electrodes. These effects can be related to two different conditions: (i) variable distribution of ionic and electronic components of the current within the electrodes and (ii) complexity of the mass transfer process in the porous mass, which may produce a slight bending in the middle part of the polarization curve, as proved by many mathematical models accounting for diffusion in the porous mass [35]. However, these contributions are very small for the thin catalytic layers usually employed in PEMFC.

The computation of the total fitting equation is carried out according to the previous scheme. To illustrate the interesting results thus obtained, the steps described in the previous sections can be summarized as follows:

1. The linear fitting of the first part of the V/log ($|i|$) plot provides the values of the exchange current density i_0 and cathodic transfer coefficient α_{cat} for oxygen reduction. Then the activation overpotential for ORR is computed using Eq. (2), which is numerically inverted to obtain $\eta_{act,O_2}(i)$.
2. The open circuit voltage is evaluated by computing the mixed potential on the basis an arbitrary oxidation reaction, Eq. (7). This allows the determination of an estimate of the hydrogen crossover current density.
3. The value of the exchange current density for HOR is obtained and the corresponding activation overpotential is computed by Eq. (2), which is inverted to provide $\eta_{act,H_2}(i)$.
4. The fitting for the ohmic resistance value is carried out employing the relationship $R(I) = R_0 (1 + aI^n)$.
5. Finally the concentration overpotentials are computed, based on the known values of the stoichiometric coefficients for hydrogen and oxygen.

Having computed all necessary terms, the $V(i)$ curve is obtained according to Eq. (1).

Fig. 5, which refers to the polarization data of Test 3 in Fig. 7, illustrates one example of such analysis. Together with the experimental data and the total fitting equation (curve e), also single terms are plotted in sequence in Fig. 5 as: curve a: $E_{rev} - \eta_{act,O_2}$; curve b: $E_{rev} - (\eta_{act,O_2} + \eta_{act,H_2})$;
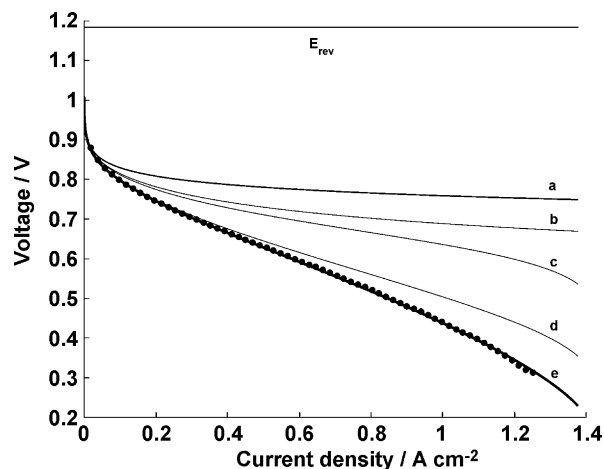

Fig. 5. Analysis of the polarization curve corresponding to Test 3 shown in Fig. 7. ElectroChem Inc. MEA, 5 cm^2, 1 mg Pt cm^{-2}, $T = 70\,^\circ$C, humidified H$_2$ and O$_2$ (100% RH) at atmospheric pressure, H$_2$ stoichiometry flow 1.5, O$_2$ stoichiometry flow 2. The letters from a to d refer to the various computed polarizations (activation overpotential for oxygen reduction, for hydrogen oxidation, concentration overpotential and ohmic drop). Curve e is the total fitting equation.

curve c: $E_{rev} - (\eta_{act,O_2} + \eta_{act,H_2} + \eta_{conc,O_2} + \eta_{conc,H_2})$; curve d: $E_{rev} - (\eta_{act,O_2} + \eta_{act,H_2} + \eta_{conc,O_2} + \eta_{conc,H_2} + R_0 i)$; curve e: $E_{rev} - [\eta_{act,O_2} + \eta_{act,H_2} + \eta_{conc,O_2} + \eta_{conc,H_2} + R(i) \times i]$.

In order to compare the catalytic behavior of different MEAs, on the basis of the analysis of the polarization curves, a parameter suitable for the evaluation of the catalyst activity for ORR has been defined as the current density at the overpotential $|\eta| = 0.3$ V ($i_{\eta=0.3}$). Similar definitions have been proposed in the literature [36], the present one does not refer to a cell voltage value (typically 0.9 V), because different temperature and gas pressure conditions may change the reversible cell voltage, so the choice of an overvoltage value ($V_{rev} - V$) appears more appropriate. The proposed parameter is obtained on the computed curve $E_{rev} - \eta_{act,O_2}$, where the activation overpotential for oxygen reduction is only considered. In this way the estimate of the catalytic activity does not depend on the other dissipation terms, particularly the ohmic resistance, which may markedly affect the MEA performance. For Test 2 described in Fig. 7, we found a value $i_{\eta=0.3} = 19.2$ mA cm^{-2}, as illustrated in Fig. 6. Having examined numerous tests with laboratory prepared and commercial MEAs, we may affirm that this parameter can be very effective in comparing the ORR catalytic activity.

The analysis described in this paper has been performed on various tests corresponding to different performance of laboratory prepared MEAs and commercial MEAs. As an example the results obtained by analyzing three different tests, chosen
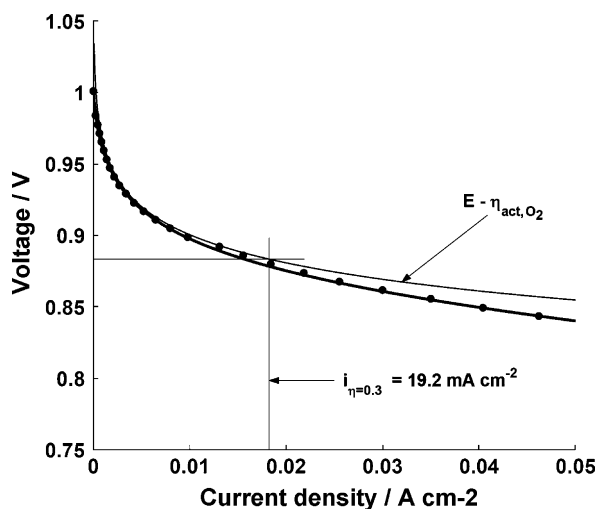
Fig. 6. Determination of the parameter ($i_{\eta=0.3}$) assumed to quantify the catalytic activity for ORR. The data refer to test 2 in Fig. 7.
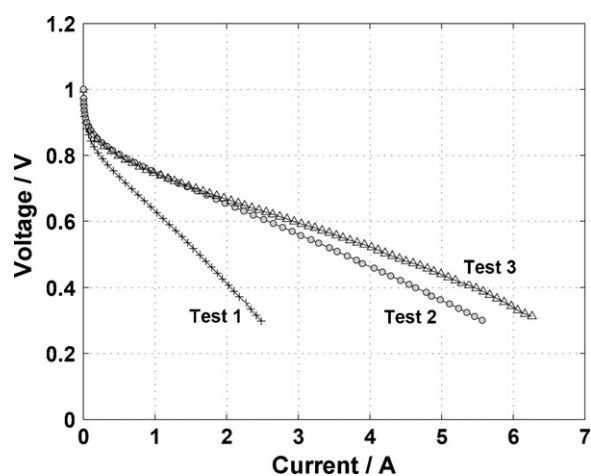

Fig. 7. Plot of three polarization curves obtained on different MEAs, analysed in the paper. Tests 1 and 2 refer to laboratory prepared MEAs of 5 cm^2, with a Pt load of 0.5 mg cm^{-2}, humidified H$_2$ and O$_2$ (Test 1: 60% RH and Test 2: 100% RH) at atmospheric pressure, stoichiometry flow 2. Test 3 refer to a commercial MEA by ElectroChem Inc., 5 cm^2, 1 mg Pt cm^{-2}, $T = 70\,^\circ$C, humidified H$_2$ and O$_2$ (100% RH) at atmospheric pressure, H$_2$ stoichiometry flow 1.5, O$_2$ stoichiometry flow 2.

because of markedly different performances (Fig. 7) are shown in Table 1. All three tests were carried out with MEAs of 5 cm^2. Tests 1 and 2 refer to laboratory prepared MEAs (as indicated in the experimental section) with a Pt load of 0.5 mg cm^{-2}, the resistance value for Test 1 is very high, compared to the one of Test 2, because this test was performed under low humidification conditions (60% RH). Test 3 refer to a commercial MEA by ElectroChem Inc., with 1 mg cm^{-2} of Pt.

4. Conclusion

A simplified model is proposed to analyse polarization curves of single PEMFC, by computing the different overpotential components which provide the best fitting of the experimental data.

The open circuit potential for the oxygen electrode, which is known to be markedly lower than the reversible potential, is interpreted in terms of mixed potential, assuming an arbitrary parasitic oxidation reaction. This allows a very good fitting of the polarization data at extremely low current densities. In addition, from the value of the current density of the parasitic reaction at the open circuit potential, a good estimate of the hydrogen crossover can be obtained. This is confirmed by literature data.

A parameter for the evaluation of the electrocatalytic performance of the ORR is introduced. It is defined as the value of the current density for a cathode overpotential of 0.3 V ($i_{\eta=0.3}$) computed on the theoretical curve for the activation overpotential of the ORR.

The possible change of the ohmic resistance with current intensity is accounted for and discussed.

The results of three polarization tests performed on laboratory prepared and commercial MEAs exhibiting different performances have been analysed with the proposed method, which appears to be an effective tool for the evaluation of MEA performance.

References

[1] P. Costamagna, S. Srinivasan, J. Power Sources 102 (2001) 253.
[2] S. Gamburzev, A.J. Appleby, J. Power Sources 107 (2002) 5.
[3] E. Antolini, J. Appl. Electrochem. 34 (2004) 563.
[4] A. Kraytsberg, Y. Ein-Eli, J. Power Sources 160 (2006) 194.
[5] J.R.C. Salgado, E. Antolini, E.R. Gonzalez, J. Power Sources 141 (2005) 13.
[6] B. Wang, J. Power Sources 152 (2005) 1–15.
[7] H.A. Gasteiger, J.E. Panels, S.G. Yan, J. Power Sources 127 (2004) 162.
[8] J. Marie, S. Berthon-Fabry, P. Achard, M. Chatenet, A. Pradourat, E. Chainet, J. NonCryst. Solids 350 (2004) 88.
[9] F. Jaouen, F. Charreteur, J.P. Dodelet, J. Electrochem. Soc. 153 (2006) A689.
[10] U.A. Paulus, A. Wokaun, G.G. Scherer, T.J. Schmidt, V. Stamenkovic, N.M. Markovic, P.N. Ross, Electrochim. Acta 47 (2002) 3787.
[11] Z.N. Farhat, J. Power Sources 138 (2004) 68.
[12] J. Jiang, B. Yi, J. Electroanal. Chem. 577 (2005) 107.
[13] C. Médard, M. Lefèvre, J.P. Dodelet, F. Jaouen, G. Lindbergh, Electrochim. Acta 51 (2006) 3202.
[14] N. Travitsky, T. Ripenbein, D. Golodnitsky, Y. Rosenberg, L. Burshtein, E. Peled, J. Power Sources 161 (2006) 782.
[15] W. Xu, X. Zhou, C. Liu, W. Xing, T. Lu, Electrochem. Commun. (2007) 1002.
[16] V.A. Paganin, E.A. Ticianelli, E.R. Gonzalez, J. Appl. Electrochem. 26 (1996) 297.
[17] S.J. Shin, J.K. Lee, H.Y. Ha, S.A. Hong, H.S. Chun, I.H. Oh, J. Power Sources 106 (2002) 146.
[18] L. Xiong, A. Manthiram, Electrochim. Acta 50 (2005) 3200.
[19] C. Francia, M. Lucariello, N. Penazzi, I. Rosso, G. Gianolio, Proceedings of the Congress "Fuel Cells Science and Technology 2004, Scientific Advances in Fuel Cell Systems, Munich, Germany, October 6–7th, 2004.
[20] L. Pisani, G. Murgia, M. Valentini, B. D'Aguanno, J. Power Sources 108 (2002) 192.
[21] M.V. Williams, H. Russell Kunz, J.M. Fenton, J. Electrochem. Soc. 152 (2005) A635.
[22] H.A. Gasteiger, W. Gu, R. Makharia, M.F. Mathias, B. Sompalli, Beginning-of-Life MEA performance—efficiency loss contributions, in: W. Vielstich, A. Lamm, H.A. Gasteiger (Eds.), Handbook of Fuel Cells:

Fundamentals, Technology, and Applications, vol. 3, John Wiley & Sons, New York, 2003, pp. 593–610 (Part 1, Chapter 46).

[23] K.C. Neyerlin, H.A. Gasteiger, C.K. Mittelsteadt, J. Jorne, W. Gu, J. Electrochem. Soc. 152 (2005) A1073.

[24] R.F. Mann, J.C. Amphlett, M.A.I. Hooper, H.M. Jensen, B.A. Peppley, P.R. Roberge, J. Power Sources 86 (2000) 173.

[25] M.R. Tarasevich, A. Sadkowski, E. Yeager, Comprehensive Treatise of Electrochemistry, in: B.E. Conway, J.O'M. Bockris, E. Yeager, S.U.M. Khan, R.E. White (Eds.), Kinetics and Mechanism of Electrode Processes, vol. 7, Plenum Press, New York, 1983, p. 306.

[26] M. Inaba, T. Kinumoto, M. Kiriake, R. Umebayashi, A. Tasaka, Z. Ogumi, Electrochim. Acta 51 (2006) 5746.

[27] S.S. Kocha, J. Deliang Yang, J.S. Yi, AIChE J. 52 (2006) 1916.

[28] M. Seddiq, H. Khaleghi, M. Mirzaei, J. Power Sources 161 (2006) 371.

[29] M. Han, S.H. Chan, S.P. Jiang, Int. J. Hydrogen Energ. 32 (2007) 385.

[30] J. Yu, T. Matsuura, Y. Yoshikawa, M.N. Islam, M. Hori, Electrochem. Solid State Lett. 8 (2005) A156.

[31] J. Zhang, Y. Tang, C. Song, J. Zhang, H. Wang, J. Power Sources 163 (2006) 532.

[32] B. Andreaus, G.G. Scherer, Solid State Ionics 168 (2004) 311.

[33] K.R. Cooper, M. Smith, J. Power Sources 160 (2006) 1088.

[34] M. Eikerling, Y.I. Kharkats, A.A. Kornyshev, Y.M. Volkovich, J. Electrochem. Soc. 145 (1998) 2684.

[35] Q. Guo, V.A. Sethuraman, R.E. White, J. Electrochem. Soc. 151 (2004) A983.

[36] H.A. Gasteiger, S.S. Kocha, B. Sompalli, F.T. Wagner, Appl. Catal. B: Environ. 56 (2005) 9.